J. Am. Soc. Mass Spectrom. (2012) 23:1191–1201
DOI: 10.1007/s13361-012-0389-8

RESEARCH ARTICLE

Gas Phase Chemistry of Li^+ with Amides: the Observation of LiOH Loss in Mass Spectrometry

Cheng Guo, Yuping Zhou, Pengyuan Liu, Yunfeng Chai, Yuanjiang Pan

Department of Chemistry, Zhejiang University, Hangzhou 310027, China

Abstract

Collision-induced dissociation (CID) of Li^+ adducts of three sets of compounds that contains an amide bond, including 2-(4, 6-dimethoxypyrimidin-2-ylsulfanyl)-*N*-phenylbenzamide, its derivatives and simpler structures was investigated by electrospray ionization tandem mass spectrometry (ESI-MS/MS). Observed fragment ions include those that reflect loss of LiOH. Other product ions result from the Smiles rearrangement and direct C–S bond cleavage. MS/MS of H/D exchange products demonstrated occurrence of a 1,3-H shift from the amide nitrogen atom to the phenyl ring of these compounds. The LiOH loss from Li^+ adducts of amides was further examined by CID of $[M + Li]^+$ ions of *N*-phenylbenzamide and *N*-phenylcinnamide. Loss of LiOH was essentially the sole fragmentation reaction observed for the former. For the latter, both losses of LiOH and H_2O were discovered. The presence of electron-donating substituents of the phenyl ring of these compounds was found to facilitate elimination of LiOH, while that loss was retarded by electron-withdrawing substituents. Proposed fragment ion structures were supported by elemental compositions deduced from ultrahigh resolution Fourier transform ion cyclotron resonance tandem mass spectrometry (FTICR-MS/MS) *m/z* value determinations. Density functional theory-based (DFT) calculations were performed to evaluate potential mechanisms for these reactions.

Key words: 2-(4,6-Dimethoxypyrimidin-2-ylsulfanyl)-*N*-phenylbenzamide, *N*-phenylbenzamide, *N*-phenylcinnamide, LiOH loss, H/D exchange, Smiles rearrangement, Theoretical calculation, Substituent effect

Introduction

ESI-MS/MS has assumed increasing importance as an invaluable tool for the study of the gas phase behaviors of biomolecules [1–3]. In the past few decades, continuous efforts have been devoted to the investigation of the dissociation reactions of charged compounds derived from protonation [4–8] or deprotonation [9–13]. On the other hand, the mass spectrometric fragmentations of metal cationized, especially lithiated biomolecules, have attracted much attention because of the desire to measure intrinsic metal ion affinity and identify the binding sites [14, 15], and because the interesting dissociation pathways exhibited by these compounds are usually different from the protonated and deprotonated analogues [16, 17]. Recently, the fragmentation behaviors of lithiated species have been reported for peptides, fatty acids, phospholipids, polytetrahydrofuran, cardiolipins, thioesters, cholesteryl esters, and disaccharides [18–26].

The amide bond forms the fundamental linkage between monomeric amino acid residues in peptide polymers, and it is important to understand its gas-phase chemistry, which has so far been studied mainly through the decomposition reactions of protonated amides and peptides [27–31]. The mobile proton model [32–37] was proposed and applied to

Electronic supplementary material The online version of this article (doi:10.1007/s13361-012-0389-8) contains supplementary material, which is available to authorized users.

Correspondence to: Yuanjiang Pan; *e-mail:* panyuanjiang@zju.edu.cn

Received: 8 February 2012
Revised: 3 April 2012
Accepted: 4 April 2012
Published online: 2 May 2012

the flexible peptides and proteins besides the rigid molecules to describe the mobility of the proton across the protonated species. In addition, the studies of the gas-phase interactions between Li^+ and peptides also have drawn a great deal of attention. Several groups [38–43] have examined the gas-phase decomposition reactions of the adduct ions in fast atom bombardment and electrospray ionization tandem mass spectrometry. However, little attention so far has been paid to the fragmentation pattern of the complexes of Li^+ with other amide-containing molecules.

One class of amides that are of interest are pesticide precursors, such as 2-(4, 6-dimethoxypyrimidin-2-ylsulfanyl)-*N*-phenylbenzamide and its derivatives [44, 45]. Here we report our studies of the gas phase chemistry of Li^+ adducts of these compounds upon ESI-MS/MS, and among the fragment ions we observe are those reflecting loss of LiOH. Product ions that reflect the Smiles rearrangement, which has been well documented in the solution phase [46, 47] as summarized in Scheme 1, and other fragmentation reactions are also observed. To further examine the elimination of LiOH from Li^+ adducts of this class of amide-containing compounds, we have also studied spectra obtained from CID of $[M + Li]^+$ ions of the simpler compounds *N*-phenylbenzamide and *N*-phenylcinnamide. The reaction mechanisms involved in formation of product ions were elucidated, and the effects of substituents on the loss of LiOH were characterized. In addition, theoretical calculations based on DFT method were performed to evaluate the proposed mechanisms.

Experimental

Mass Spectrometry

The samples were first analyzed in positive ion mode on a Varian 500-MS ion trap mass spectrometer equipped with an electrospray ionization (ESI) source, with data acquisition using the Varian MS Workstation (Varian, Palo Alto, CA, USA). The compounds were dissolved in methanol in normal collision-induced dissociation experiment or dissolved in methanol-d4 in the D-labeling experiment, and then lithium chloride solution was added to the sample solutions. The samples were infused into the source chamber at a flow rate of 10 μL min^{-1} with the following parameters: spray chamber temperature, 50 °C; needle voltage, 5000 V; spray shield voltage, 600 V; capillary voltage, 80 V; rf loading, 80 %; scan mode, standard; drying gas temperature, 300 °C. Nitrogen was used as the drying gas at a pressure of 15 psi and the nebulizing gas at a pressure of 35 psi. Tandem mass spectra were obtained by CID with helium as the collision gas after isolation of the desired precursor ion and the isolation window was set as 1.0 *m/z* unit. The excitation amplitude (resonance mode) was set to give suitable energy for the dissociation of all compounds.

All accurate mass spectrometric experiments were carried out on an Apex III (7.0 Tesla) FTICR mass spectrometer (Bruker, Billerica, MA, USA). XMASS software version 6.1.1 (Bruker) was used for instrument control, data acquisition, and processing. Sodium trifluoroacetate was used as an external calibration compound. Solutions were infused from the ESI source at 3 μL min^{-1} with parameters: capillary, –4269 V; end plate, –3803 V; skimmer 1, 12.00 V; skimmer 2, 6.61 V; offset, 0.98 V; rf amplitude, 582.5 Hz; drying gas temperature, 150 °C. Nitrogen was used as the nebulizing and drying gas, and argon was used as the collision gas. MS/MS analysis was performed through isolation of the desired precursor ion using a correlated sweep. Sustained off-resonance irradiation (SORI) was applied for CID. The pulse parameters were set as follows: correlation sweep pulse length, 1000 μs; correlation sweep attenuation, 12 dB; ejection safety belt, 1000 Hz; ion activation pulse length, 250,000 μs; ion activation attenuation, 43 dB; frequency offset from activation mass, 600 Hz; user delay length, 3 s.

Theoretical Calculations

All theoretical calculations were carried out by using the DFT method (a quantum mechanical modeling method used in physics and chemistry to investigate the electronic structure (principally the ground state) of many-body systems, in particular atoms, molecules, and ions) at the B3LYP/6-31++G(d,p) level of theory in the Gaussian 03 program [48]. The candidate structures of the reactants, products, intermediates, and transition states were optimized by calculating the force constants. No symmetry constrains were imposed in the optimizations. The reaction pathways were traced forward and backward by the intrinsic reaction coordinate (IRC) method. All optimized structures were subjected to vibrational frequency analysis for zero-point energy (ZPE) correction. The sum of electronic and thermal energies of the optimized structures was discussed.

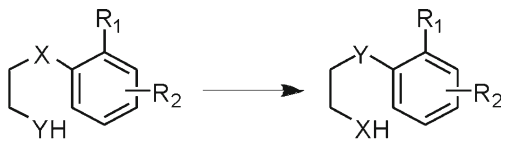

Scheme **1.** Classic example of Smiles rearrangement

Results and Discussion

Investigation of the Fragmentation of the Lithiated 2-(4, 6-Dimethoxypyrimidin-2-Ylsulfanyl)-N-Phenylbenzamide and Its Derivatives

The structures of 2-(4, 6-dimethoxypyrimidin-2-ylsulfanyl)-*N*-phenylbenzamide and its derivatives are listed in Table 1. Generally, all the compounds gave similar fragmentation,

Table 1. Relative Abundances of Product Ions in the CID Spectra of $[M + Li]^+$ Ions of 2-(4, 6-dimethoxypyrimidin-2-ylsulfanyl)-*N*-phenylbenzamide and Its Derivatives (Excitation Amplitude is 1.20 V)

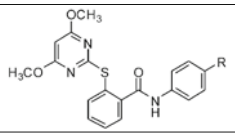

Compound	R	$[M + Li]^+$	$C_{19}H_{15}O_2N_3SR^+$	$C_{12}H_{14}O_3N_3LiR^+$	$C_{12}H_{12}O_2N_3LiR^+$	$C_6H_7O_2N_2^+$
1	H	374 (23.9)[a]	350 (12.6)	256 (3.8)	238 (100)	139 (10.2)
2	$N(CH_3)_2$	417 (32.7)	393 (19.0)	299 (0.3)	281 (100)	139 (1.0)
3	OCH_3	404 (47.7)	380 (16.9)	286 (2.3)	268 (100)	139 (4.2)
4	CH_3	388 (49.1)	364 (14.2)	270 (2.5)	252 (100)	139 (2.8)
5	F	392 (100)	368 (11.5)	274 (9.1)	256 (89.3)	139 (2.3)
6	Cl	408 (100)	384 (7.6)	290 (8.5)	272 (63.3)	139 (13.2)
7	Br	452 (100)	428 (4.1)	334 (4.7)	316 (44.1)	139 (3.0)

[a] *m/z* (relative abundance, %)

whereas the nature of the substituents merely affected the relative abundances (RAs) of the product ions.

Compound **1** is selected as a model to demonstrate the possible fragmentation pathways. Theoretical calculations indicate that the carbonyl oxygen is the most thermodynamically favored site for Li^+ complexation because that molecular ion has the lowest energy (Table S1). The full scan mass spectrum of Compound **1** shows an abundant lithiated molecule at *m/z* 374. Upon collisional activation, it yields four product ions at *m/z* 139, 238, 256, and 350, as shown in Figure 1a. The formation of these fragment ions can be rationalized by the reaction mechanism described in Scheme 2. The base peak (ion **b** at *m/z* 238) was produced by the Smiles rearrangement [49] reaction (the nucleophilic attack of the amide nitrogen atom to the pyrimidine carbon atom). Ion **c** is 18 Da more than ion **b**, and it was confirmed

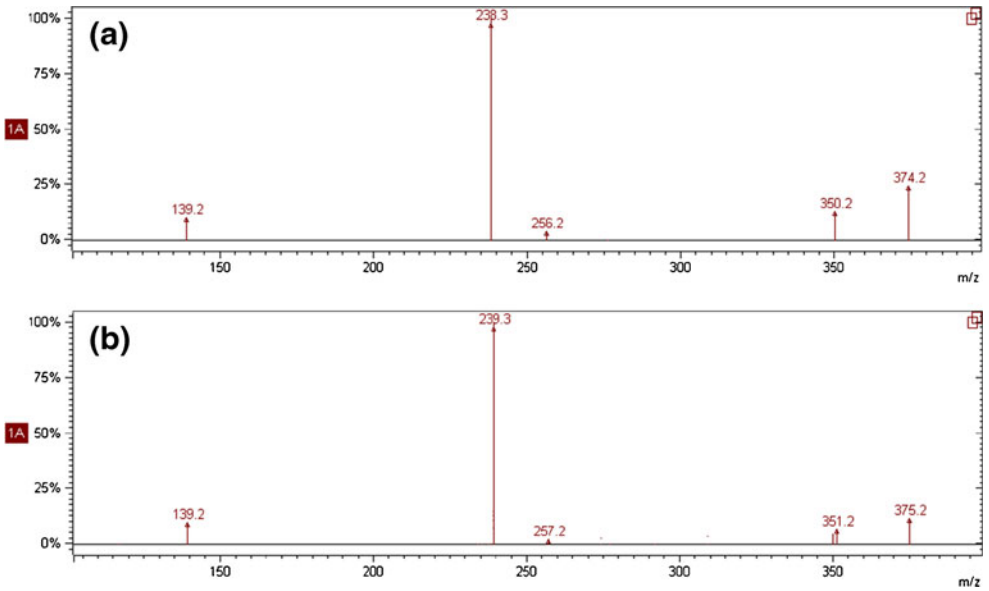

Figure 1. The CID mass spectra of $[M + Li]^+$ ions of (**a**) Compound 1 and (**b**) deuterated Compound 1

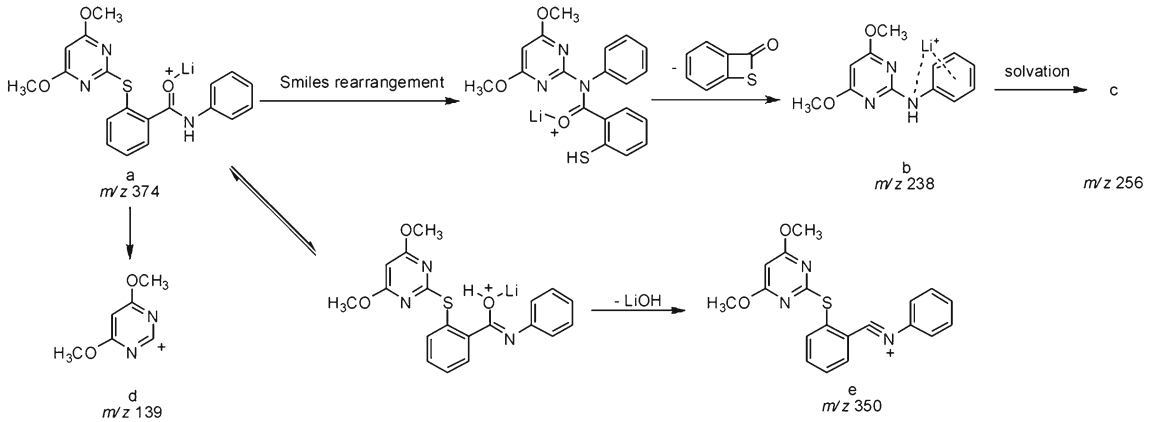

Scheme **2.** Proposed fragmentation mechanism of the $[M + Li]^+$ ion of 2-(4, 6-dimethoxypyrimidin-2-ylsulfanyl)-*N*-phenylbenzamide

by FTICR-MS/MS that ion **c** resulted from the solvation [24] of the ion **b** (Table S2). Ion **d** at *m/z* 139, 4,6-dimethoxypyrimidin ion, was produced by the direct cleavage of C–S bond. Another interesting fragmentation pathway involved the elimination of 24 Da, which was confirmed to be LiOH from the precursor ion. In 1990, Larrivee and Allison [50] examined gas phase fragmentation reactions of Li^+ adducts of α,ω-bifunctional alkanes and observed that hydroxylated compounds could undergo loss of LiOH, but such losses from Li^+ adducts of amides has not yet been reported to our knowledge.

Isotope labeling is always powerful in the studies of reaction mechanisms, and D-labeling experiments were carried out. The CID mass spectrum of the lithiated deuterated Compound **1** is shown as Figure 1b. Upon collisional activation after H/D exchange, interestingly, the ions at *m/z* 350 and 351 were both observed, and the formulas were confirmed to be $C_{19}H_{16}O_2N_3S^+$ and $C_{19}H_{15}O_2N_3SD^+$, respectively (Table S2). The existence of ion at *m/z* 351, which results from the loss of LiOH, implies that the deuteron migrates to the phenyl ring and exchanges with the proton on the phenyl ring. In fact, the proton transfer and H/D exchange processes of protonated aromatics have been studied in the past decades [51–62]. After the deuteron transfers from the nitrogen to one of the *ortho*-positions of the phenyl ring, the proton may migrate back to the nitrogen while the deuteron retains on the phenyl ring [63, 64], which allows the interconversion of **f-1** and **f-2** via **g**. The subsequent loss of LiOD from **f-1** or LiOH from **f-2** results in the formation of the ion at *m/z* 350 or 351, respectively. The proposed mechanism is shown in Scheme 3.

The fragmentation mechanisms could be further explored by studying the substituent effects on the distribution of the product ions and the spectra of a series of compounds with different substituents at *para* position of the N-linked phenyl ring were measured. A plot of the abundance ratio of these

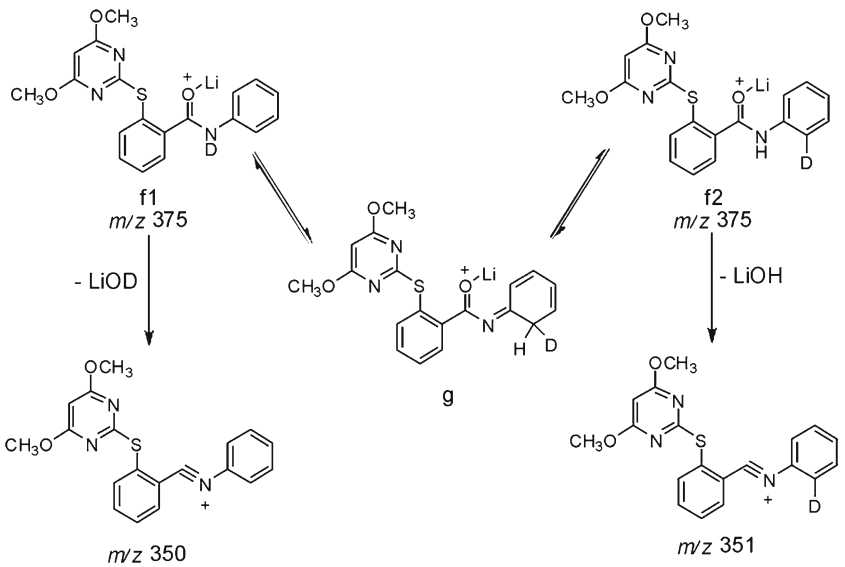

Scheme **3.** Proposed mechanism to explain the losses of LiOD and LiOH from $[M + Li]^+$ ion of deuterated 2-(4,6-dimethoxypyrimidin-2-ylsulfanyl)-*N*-phenylbenzamide

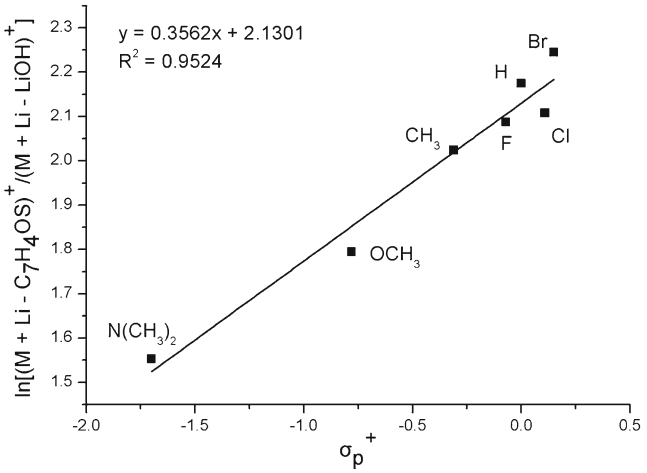

Figure 2. Plot of $\ln[(M + Li - C_7H_4OS)^+/(M + Li - LiOH)^+]$ vs the σ_p^+ substituent constants for the collision-induced fragmentation of the lithiated *para*-monosubstituted 2-(4,6-dimethoxypyrimidin-2-ylsulfanyl)-*N*-phenylbenzamides. Excitation amplitude is 1.20 V (helium)

two ions, $\ln[(M + Li - C_7H_4OS)^+/(M + Li - LiOH)^+]$ (the ion at *m/z* 139 is not considered because the substituents are too distant to affect its formation) versus the substituent constants, σ_p^+, was obtained as shown in Figure 2. The trend clearly indicates that the electron-donating substituents expedited the loss of LiOH, whereas the electron-withdrawing groups retarded the loss. In the reaction of the LiOH loss, a positive charge is developing at the carbon atom connecting the substituted N-linked phenyl ring. An electron-donating substituent (e.g., OCH_3 or NMe_2) reduces the overall activation barrier of the transition state, and the product ion is stabilized by delocalization of the positive charge at the carbon atom over the substituted phenyl ring system. This favors elimination of LiOH from $[M + Li]^+$ ion relative to Compound **1**. In contrast, an electron-withdrawing substituent destabilized the product ion, and the overall activation barrier of the transition state is increased, which militates against elimination of LiOH. In addition, electron-withdrawing moieties have previously been demonstrated to

Table 2. Relative Abundances of Product Ions in the CID Spectra of $[M + Li]^+$ Ions of *N*-phenylbenzamide and Its Derivatives (Excitation Amplitude is 0.50 V)

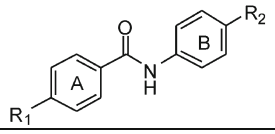

Compound	R_1	R_2	$[M + Li]^+$	$[M + Li - LiOH]^+$
8	H	H	204 (100)[a]	180 (36.9)
9	OCH_3	H	234 (91.3)	210 (100)
10	CH_3	H	218 (100)	194 (51.5)
11	Cl	H	238 (100)	214 (4.8)
12	Br	H	282 (100)	258 (1.6)
13	H	OCH_3	234 (100)	210 (74.8)
14	H	CH_3	218 (100)	194 (40.1)
15	H	Cl	238 (100)	214 (5.1)
16	H	Br	282 (100)	258 (2.4)

[a] *m/z* (relative abundance, %)

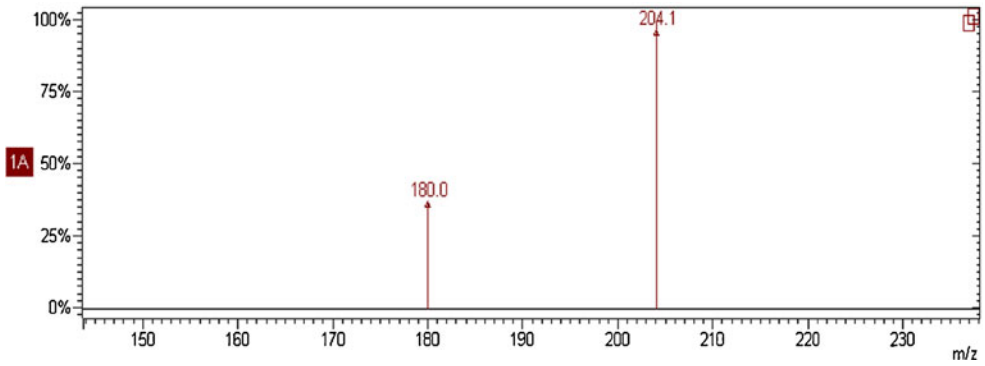

Figure 3. The CID mass spectrum of $[M + Li]^+$ ion of Compound 8

favor the Smiles rearrangement reaction [49]. These two factors cause elimination of LiOH from $[M + Li]^+$ ion to be less favorable for compounds with electron-withdrawing substituents.

Investigation of the Fragmentation of the Lithiated N-Phenylbenzamide and Its Derivatives

To further explore the interaction of Li^+ with amide-containing biomolecules and the elimination of LiOH from such adduct ions, we examined the fragmentation of simpler compounds, including *N*-phenylbenzamide and its derivatives. Effects of A- and B-ring substituents on this loss were also investigated. The structures of these compounds and their major product ions from CID of $[M + Li]^+$ ions with their RAs are summarized in Table 2.

CID of $[M + Li]^+$ of *N*-phenylbenzamide (Compound **8**) produced the sole fragment ion at *m/z* 180, as shown in Figure 3, by the putative mechanism proposed in Scheme 4. The proposed mechanism was examined further by obtaining CID spectrum after H/D exchange, as illustrated in Figure S1. As expected, fragment ions at *m/z* 180 and 181 were observed that reflected loss of LiOD and LiOH (Table S2), respectively, and their formation is proposed to occur by the mechanism illustrated in Scheme S1.

To exclude the possibility that the H atom in the eliminated LiOH arises from direct transfer from the phenyl ring, fragmentation of $[M + Li]^+$ of Compound **17** (Scheme 5) was studied (Figure S2a). In this case, the H atom bonded to the amide nitrogen atom is replaced with a methyl group. It proved to be difficult to induce fragmentation of the precursor ion even at high collision energies, and the loss of LiOH was not discovered. To examine this issue further, CID of $[M + Li]^+$ of Compound **18** was performed after H/D exchange. In Compound **18,** the H atoms at both *ortho*-positions of the N-linked phenyl ring are replaced by Cl. In this case, losses of LiOD and LiCl were observed, but loss of LiOH was not (Figure S2b). This implies that the hydrogen ring-walk [65] (it means that the deuteron migrated to the *ortho*-position will further exchange with the protons at the *meta*-positions and *para*-position) following the 1,3-H shift does not take place.

Theoretical calculations were performed to evaluate the proposed mechanism and the possible involvement of a transition state and its intermediate in the loss of LiOH. A schematic potential energy surface for the proposed mechanism is shown in Figure S3 that describes the energy requirement of the reactions quantitatively.

Theoretical computations indicate that the carbonyl oxygen is the most favorable site for Li^+ complexation to yield the MLi-a ion depicted in Scheme 4, which is in equilibrium with the tautomer MLi-b. The positive charge induces cleavage of the C–O bond via transition state a (TSa) and formation of an ion-neutral complex a (INC-a). Elimination of LiOH from INC-a results in product ion **A** (Scheme 4). The optimized structures, the lengths of important bonds (in Angstroms) and

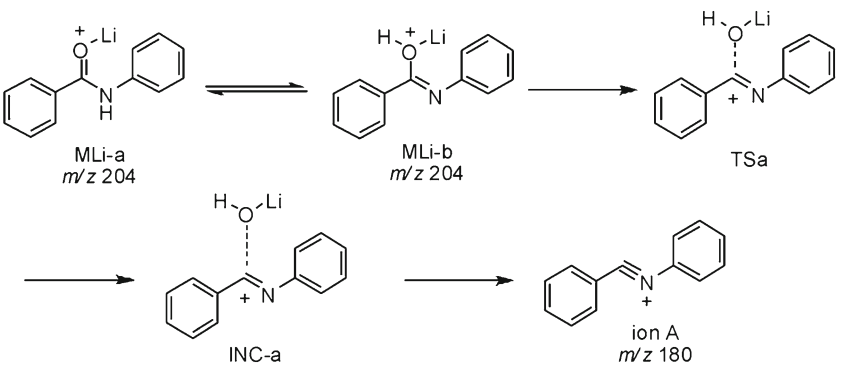

Scheme **4.** Proposed mechanism to explain the loss of LiOH from $[M + Li]^+$ ion of *N*-phenylbenzamide

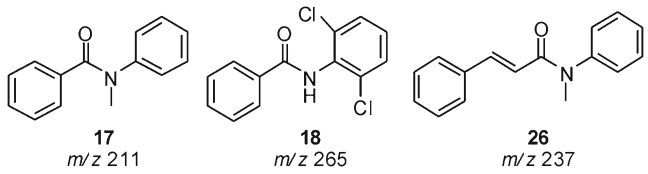

Scheme **5.** Structures of Compounds 17, 18, and 26

the calculated heats of formation of species involved in this reaction are illustrated in Figure 4.

Theoretical calculations were performed to evaluate substituent effects on the activation barrier and the stability of product ions. For compounds with electron-donating groups (e.g., Compound **9**), which contains the electron-donating A-ring substituent OCH_3, the energy of the TSa (51.6 kcal/mol) is lower than that of Compound **8**. In addition, the product ion is stabilized by delocalization of the positive charge over the OCH_3-substituented aromatic ring. These two factors cause the loss of LiOH to be more favorable for Compound **9** relative to Compound **8**. These theoretical calculations yield predictions that are consistent with the experimental findings (Table 2). In contrast, compounds with electron-withdrawing groups [e.g., Compound **12** (which has an A-ring Br substituent)], exhibits an energy barrier of the TSa (52.8 kcal/mol) that is higher than that of Compound **8**. Moreover, the product ion cannot readily be stabilized by delocalization of the positive charge. Consequently, loss of LiOH is less favorable for Compound **12** than for Compound **8**. Similar results were obtained for compounds substituted on the B-ring (Table 2).

Investigation of the Fragmentation of the Lithiated N-Phenylcinnamide and Its Derivatives

The structures of *N*-phenylcinnamide and its derivatives and their major product ions with their RAs are summarized in Table 3. CID of $[M + Li]^+$ of these compounds resulted in similar fragmentation pattern that included losses of LiOH and H_2O. CID of $[M + Li]^+$ of the prototype *N*-phenylcinnamide (Compound **19**) produced two major fragment ions at *m/z* 206 and 212 (Figure 5), and their formation is rationalized by the competitive reactions illustrated in Scheme 6.

Figure S4 illustrates the CID spectrum of $[M + Li]^+$ of Compound **19** after labeling by H/D exchange, and it contains product ions at *m/z* 207 and 213 in addition to those at *m/z* 206 and 212 that arise from loss of LiOH and H_2O, respectively (Table S2). This reflects H/D exchange between the H atom on the amide nitrogen atom and an H atom of the phenyl ring via a 1,3-H shift by the putative mechanism proposed in Scheme S2. In addition, CID of $[M + Li]^+$ of Compound **26** [in which the H atom on the amide nitrogen is replaced by a methyl group (Scheme 5)] did not result in loss of either LiOH or H_2O (Figure S5). This observation implies that the amide H atom is required for loss of LiOH and H_2O, and the observation excludes the possibility that direct transfer of an H atom from the phenyl ring or the vinyl carbon to the amide carbonyl oxygen results in loss of LiOH.

Theoretical calculations yielded a schematic potential energy surface for these reactions illustrated in Figure 6, which describes the energy requirement quantitatively. As indicated above, the carbonyl oxygen is the most favorable site for Li^+ complexation, which results in formation of the ion MLi-c in Scheme 6 that is in equilibrium with its tautomer MLi-d. As proposed in Route 1, the fragmentation pathway of elimination of LiOH via transition state 1 (TS1) (52.3 kcal/mol) is similar to that of *N*-phenylbenzamide. Figure S6 illustrates the optimized structures, the lengths of important bonds (in Angstroms) and the calculated heats of formation of species involved in the loss of LiOH. In Route 2, MLi-d rotates to generate a conformer MLi-e through

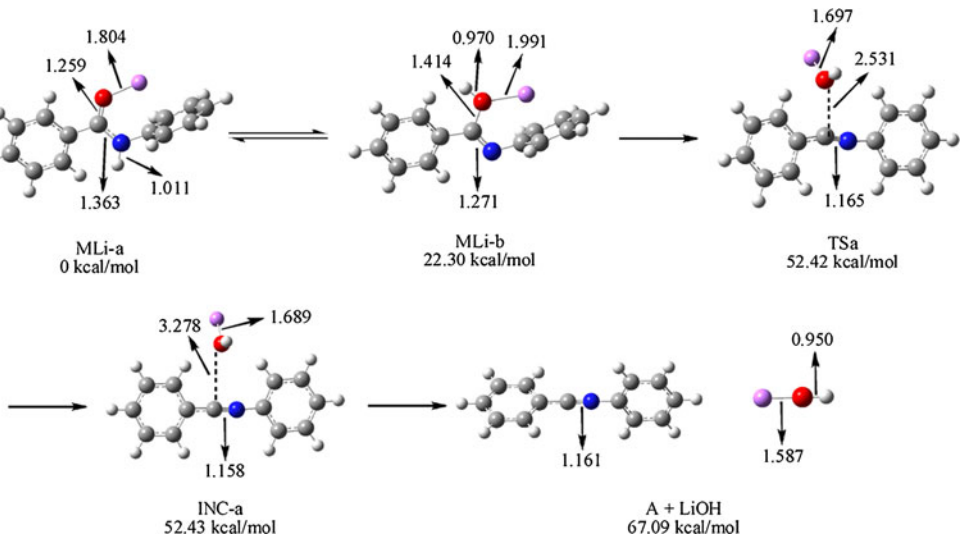

Figure 4. DFT optimized structures of the species in the reaction of losing LiOH of lithiated *N*-phenylbenzamide. Heats of formation are given kcal/mol and the lengths of the chemical bonds are given in Angstroms

Table 3. Relative Abundances of Product Ions in the CID Spectra of $[M + Li]^+$ Ions of *N*-phenylcinnamide and its Derivatives (Excitation Amplitude is 0.90 V)

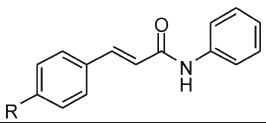

Compound	R	$[M + Li]^+$	$[M + Li - H_2O]^+$	$[M + Li - LiOH]^+$
19	H	230 (76.5)[a]	212 (23.7)	206 (100)
20	$N(CH_3)_2$	273 (7.7)	255 (2.7)	249 (100)
21	OCH_3	260 (23.3)	242 (6.2)	236 (100)
22	CH_3	244 (38.7)	226 (12.1)	220 (100)
23	F	248 (75.4)	230 (19.8)	224 (100)
24	Cl	264 (100)	246 (22.8)	240 (97.3)
25	Br	308 (100)	290 (9.4)	284 (35.1)

[a] *m/z* (relative abundance, %)

transition state 2 (TS2) first and the energy barrier is 29.9 kcal/mol, then the transfer of the proton from the carbon adjacent to the carbonyl to the oxygen through a four-membered-ring transition state 3 (TS3), which is 57.7 kcal/mol, leads to the formation of an ion-neutral complex c (INC-c). The decomposition of the INC-c leads to the loss of H_2O and the formation of ion **C**. This also implies that the proton transfer reaction is the rate determining step. Alternatively, the proton may transfer from the carbon which is adjacent to the carbonyl to the nitrogen, leading to the formation of MLi-f through a four-membered-ring transition state 4 (TS4) first. Then the proton migrates from the nitrogen to the carbonyl oxygen, leading to the cleavage of C–O bond through another four-membered-ring transition state 5 (TS5). The activation barriers of these two 1,3-H shift processes are 95.1 kcal/mol and 104.3 kcal/mol, respectively and they are much higher than these of TS2 and TS3. This indicates that the stepwise proton transfer reaction through TS4 and TS5 is less accessible in terms of energy. The optimized structures, the lengths of important bonds (in Angstroms) and the calculated heats of formation of species involved in this reaction are reported in Figure S7.

The spectra of a series of compounds with different substituents at *para* position of the phenyl ring were measured to study the substituent effects on the fragmentation systematically. And a plot of the abundance ratio of these two ions, $\ln[(M + Li - H_2O)^+/(M + Li - LiOH)^+]$ versus the substituent constants, σ_p^+, was obtained as shown in Figure S8. The trend clearly indicates that the electron-

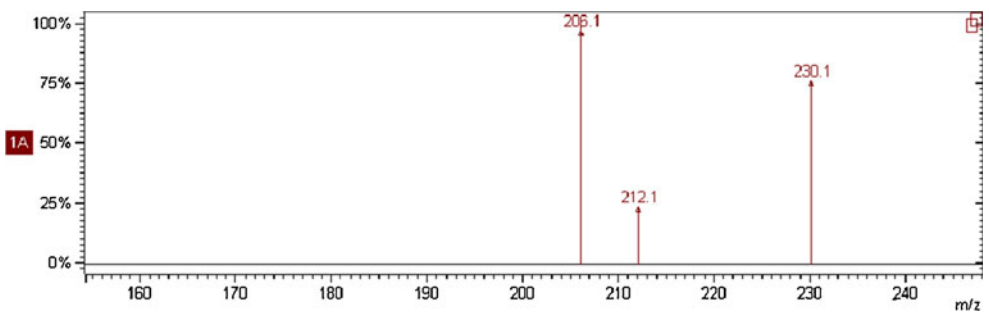

Figure 5. The CID mass spectrum of $[M + Li]^+$ ion of Compound 19

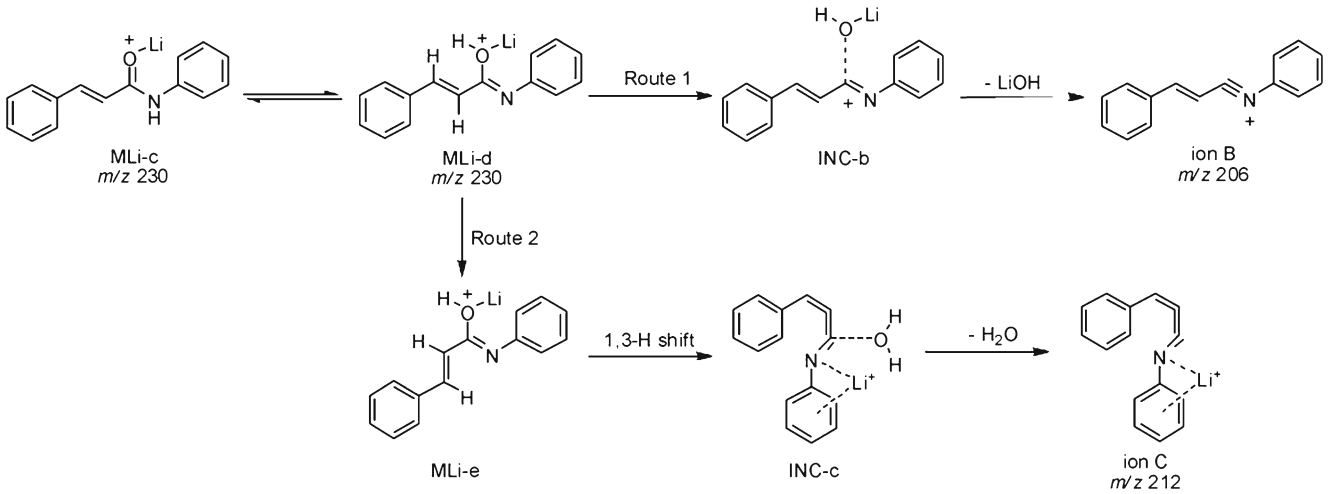

Scheme **6.** Proposed fragmentation mechanism of the $[M + Li]^+$ ion of *N*-phenylcinnamide

donating substituents were in favor of the elimination of LiOH, whereas the electron-attracting substituents favored the loss of H_2O. As elucidated before, for compounds with electron-donating substituents, the energy of TS1 is reduced and the product ion is stabilized in Route 1, while the situation is opposite for compounds with electron-withdrawing substituents. In addition, the positive charge in the reaction of losing water mainly concentrates on the lithium cation and can not resonate to the substituted phenyl ring system, which means the energy of TS3 and the stability of product ion are less affected by the substituents. For example, Compound **19** (R = H) yielded $[M + Li - LiOH]^+$ ion and $[M + Li - H_2O]^+$ ion in the ratio 100:23.7 (Figure 5); Compound **20** (R = $N(CH_3)_2$) yielded these two ions in the ratio 100:2.7 (Figure S9a) and in the case of Compound **25** (R = Br), the ratio of *m/z* 284 to 290 is 100:26.8 (Figure S9b).

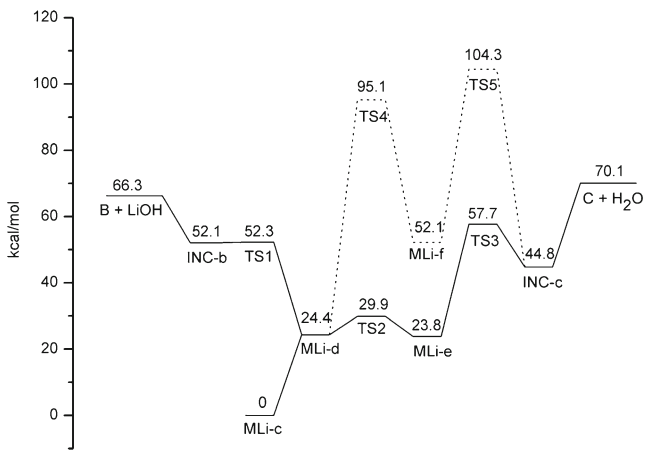

Figure 6. Schematic potential energy surface (relative energies are given in kcal/mol) for the reaction of lithiated *N*-phenylcinnamide, calculated by DFT at the B3LYP/6-31 G++(d,p) level

Conclusions

The gas phase chemistry of Li^+ with pesticides precursor 2-(4, 6-dimethoxypyrimidin-2-ylsulfanyl)-*N*-phenylbenzamide was studied by ESI-MS/MS and FTICR-MS/MS first, and then *N*-phenylbenzamide and *N*-phenylcinnamide which have simpler structures were investigated to get a better understanding. The compounds studied in each series showed similar fragmentation pathways and the loss of LiOH was observed. The H/D exchange between the H atom attached to amide nitrogen and an H atom of the phenyl ring via a 1,3-H shift was witnessed by the D-labeling experiments. The effects of substituent on the LiOH loss from the lithiated molecules were also investigated. The presence of electron-releasing groups expedited the loss of LiOH, whereas the electron-attracting groups retarded the loss. DFT theoretical calculations were also carried out to further investigate the reaction mechanisms.

Acknowledgments

The authors gratefully acknowledge the financial support from the Natural Science Foundation of China (grants no. 20975092, 21025207).

References

1. Paizs, B., Suhai, S.: Fragmentation Pathways of Protonated Peptides. *Mass Spectrom. Rev.* **24**, 508–548 (2005)
2. Chait, B.T.: Mass Spectrometry: Bottom-Up or Top-Down? *Science* **314**, 65–66 (2006)
3. Palumbo, A.M., Smith, S.A., Kalcic, C.L., Dantus, M., Stemmer, P.M., Reid, G.E.: Tandem Mass Spectrometry Strategies for Phosphoproteome Analysis. *Mass Spectrom. Rev.* **30**, 600–625 (2011)
4. Hu, N., Tu, Y.P., Liu, Y.Q., Jiang, K.Z., Pan, Y.J.: Dissociative Protonation and Proton Transfers: Fragmentation of α, β-Unsaturated Aromatic Ketones in Mass Spectrometry. *J. Org. Chem.* **73**, 3369–3376 (2008)
5. Liu, P.Y., Hu, N., Pan, Y.J., Tu, Y.P.: Ion-Neutral Complexes Resulting from Dissociative Protonation: Fragmentation of α-Furanylmethyl Benzyl Ethers and4-N,N-Dimethylbenzyl Benzyl Ethers. *J. Am. Soc. Mass Spectrom.* **21**, 626–634 (2010)

6. Hu, N., Tu, Y.P., Jiang, K.Z., Pan, Y.J.: Intramolecular Charge Transfer in the Gas Phase: Fragmentation of Protonated Sulfonamides in Mass Spectrometry. *J. Org. Chem.* **75**, 4244–4250 (2010)
7. Chai, Y.F., Guo, C., Jiang, K.Z., Pan, Y.J., Sun, C.R.: C^{α}–C^{β} and C^{α}–N Bond Cleavage in the Dissociation of Protonated *N*-Benzyllactams: Dissociative Proton Transfer and Intramolecular Proton-Transport Catalysis. *Org. Biomol. Chem.* **10**, 791–797 (2012)
8. Harrison, A.G.: Pathways for Water Loss from Doubly Protonated Peptides Containing Serine or Threonine. *J. Am. Soc. Mass Spectrom.* **23**, 116–123 (2012)
9. Blanksby, S.J., Kato, S., Bierbaum, V.M., Ellison, G.B.: Fragmentations of Deprotonated Alkyl Hydroperoxides (ROO–) upon Collisional Activation: A Combined Experimental and Computational Study. *Aust J Chem* **56**, 459–472 (2003)
10. Huang, T.Y., Kharlamova, A., Liu, J., McLuckey, S.A.: Ion Trap Collision-Induced Dissociation of Multiply Deprotonated RNA: c/y-Ions versus (a-B)/w-Ions. *J. Am. Soc. Mass Spectrom.* **19**, 1832–1840 (2008)
11. Edelson-Averbukh, M., Shevchenko, A., Pipkorn, R., Lehmann, W.D.: Discrimination Between Peptide O-Sulfoand O-Phosphotyrosine Residues by Negative Ion Mode Electrospray Tandem Mass Spectrometry. *J. Am. Soc. Mass Spectrom.* **22**, 2256–2268 (2011)
12. George, M., Ramesh, V., Srinivas, R., Giblin, D., Gross, M.L.: Deprotonated *N*-(2,4-dinitrophenyl)amino acids undergo cyclization in solution and the gas phase. *Int J Mass Spectrom* **306**, 232–240 (2011)
13. Rifai, A., Bourcier, S., Arquier, D., Charvet, Y., Jaber, F., Bouchoux, G.: Fragmentation Reactions of Phenoxide Anions: Deprotonated Dinoterb and Related Structures. *J. Mass Spectrom.* **46**, 1079–1088 (2011)
14. Leary, J.A., Zhou, Z., Ogden, S.A., Williams, T.D.: Investigation of Gas-Phase Lithium-Peptide Adducts: Tandem Mass Spectrometry and Semiempirical Studies. *J. Am. Soc. Mass Spectrom.* **1**, 473–480 (1990)
15. Teesch, L.M., Orlando, R.C., Adams, J.: Locations of the Alkali Metal Ion in Gas-Phase Peptide Complexes. *J. Am. Chem. Soc.* **113**, 3668–3675 (1991)
16. Williams, S.M., Brodbelt, J.S.: Ms^n Characterization of Protonated Cyclic Peptides and Metal Complexes. *J. Am. Soc. Mass Spectrom.* **15**, 1039–1054 (2004)
17. Sun, C.R., Zhu, P.X., Hu, N., Wang, D.H., Pan, Y.J.: Differentiation of Lisinopril and Its RSS Diastereomer by Liquid Chromatography Combined with Collision-Induced Dissociation Mass Spectrometry. *J. Mass Spectrom.* **45**, 89–96 (2010)
18. Wang, P., Polce, M.J., Bleiholder, C., Paizs, B., Wesdemiotis, C.: Structural Characterization of Peptides via Tandem Mass Spectrometry of Their Dilithiated Monocations. *Int J Mass Spectrom* **249**, 45–49 (2006)
19. Rozman, M., Gaskell, S.J.: Noncovalent Interactions of Alkalimetal Cations with Singly Charged Tryptic Peptides. *J. Mass Spectrom.* **45**, 1409–1415 (2010)
20. Hsu, F.F., Turk, J.: Elucidation of the Double-Bond Position of Long-Chain Unsaturated Fatty Acid by Multiple-Stage Linear Ion-Trap Mass Spectrometry with Electrospray Ionization. *J. Am. Soc. Mass Spectrom.* **19**, 1673–1680 (2008)
21. Stubiger, G., Pittenauer, E., Allmaier, G.: MALDI Seamless Postsource Decay Fragment Ion Analysis of Sodiated and Lithiated Phospholipids. *Anal. Chem.* **80**, 1664–1678 (2008)
22. Kuki, A., Nagy, L., Memboeuf, A., Drahos, L., Vekey, K., Zsuga, M., Keki, S.: Energy-Dependent Collision-Induced Dissociation of Lithiated Polytetrahydrofuran: Effect of the Size on the Fragmentation Properties. *J. Am. Soc. Mass Spectrom.* **21**, 1753–1761 (2010)
23. Hsu, F.F., Turk, J.: Toward Total Structural Analysis of Cardiolipins: Multiple-Stage Linear Ion-Trap Mass Spectrometry on the $[M - 2\,H + 3Li]^+$ Ions. *J. Am. Soc. Mass Spectrom.* **21**, 1863–1869 (2010)
24. Guo, C., Hu, N., Jiang, K.Z., Chen, W.X., Wang, X.X., Pan, Y.J.: Study of Fragmentation Pathways of Lithiated α, β-Unsaturated Thioesters by Electrospray Ionization Mass Spectrometry. *Rapid Commun. Mass Spectrom.* **24**, 409–414 (2010)
25. Bowden, J.A., Albert, C.J., Barnaby, O.S., Ford, D.A.: Analysis of Cholesteryl Esters and Diacylglycerols Using Lithiated Adducts and Electrospray Ionization-Tandem Mass Spectrometry. *Anal. Biochem.* **417**, 202–210 (2011)
26. Stefan, S.E., Ehsan, M., Pearson, W.L., Aksenov, A., Boginski, V., Bendiak, B., Eyler, J.R.: Differentiation of Closely Related Isomers: Application of Data Mining Techniques in Conjunction with Variable Wavelength Infrared Multiple Photon Dissociation Mass Spectrometry for Identification of Glucose-Containing Disaccharide Ions. *Anal. Chem.* **83**, 8468–8476 (2011)
27. Lin, H.Y., Ridge, D.P., Uggerud, E., Vulpius, T.: Unimolecular Chemistry of Protonated Formamide. Mass Spectrometry and ab Initio Quantum Chemical Calculations. *J. Am. Chem. Soc.* **116**, 2996–3004 (1994)
28. Tu, Y.P., Harrison, A.G.: Fragmentation of Protonated Amides Through Intermediate Ion-Neutral Complexes: Neighboring Group Participation. *J. Am. Soc. Mass Spectrom.* **9**, 454–462 (1998)
29. Tu, Y.P.: Fragmentation of Conjugated Amides at the C–C(O) Bond in Electrospray Mass Spectrometry: a Proton-Bound Dimeric Intermediate Identified by the Kinetic Method. *Rapid Commun. Mass Spectrom.* **18**, 1345–1351 (2004)
30. Jorgensen, T.J.D., Gardsvoll, H., Ploug, M., Roepstorff, P.: Intramolecular Migration of Amide Hydrogens in Protonated Peptides upon Collisional Activation. *J. Am. Chem. Soc.* **127**, 2785–2793 (2005)
31. Bythell, B.J., Maitre, P., Paizs, B.: Cyclization and Rearrangement Reactions of a_n Fragment Ions of Protonated Peptides. *J. Am. Chem. Soc.* **132**, 14766–14779 (2010)
32. Mueller, D.R., Eckersley, M., Richter, W.J.: Hydrogen Transfer Reactions in the Formation of "Y+2" Sequence Ions from Protonated Peptides. *Org Mass Spectrom* **23**, 217–222 (1988)
33. Johnson, R.S., Krylov, D., Walsh, K.A.: Proton Mobility within Electrosprayed Peptide Ions. *J. Mass Spectrom.* **30**, 386–387 (1995)
34. Dongre, A.R., Jones, J.L., Somogyi, A., Wysocki, V.H.: Influence of Peptide Composition, Gas-Phase Basicity, and Chemical Modification on Fragmentation Efficiency: Evidence for the Mobile Proton Model. *J. Am. Chem. Soc.* **118**, 8365–8374 (1996)
35. Csonka, I.P., Paizs, B., Lendvay, G., Suhai, S.: Proton mobility in Protonated Peptides: A Joint Molecular Orbital and RRKM Study. *Rapid Commun. Mass Spectrom.* **14**, 417–431 (2000)
36. Wysocki, V.H., Tsaprailis, G., Smith, L.L., Breci, L.A.: Mobile and localized protons: a framework for understanding peptide dissociation. *J. Mass Spectrom.* **35**, 1399–1406 (2000)
37. Polfer, N.C., Oomens, J., Suhai, S., Paizs, B.: Infrared Spectroscopy and Theoretical Studies on Gas-Phase Protonated Leu-enkephalin and Its Fragments: Direct Experimental Evidence for the Mobile Proton. *J. Am. Chem. Soc.* **129**, 5887–5897 (2007)
38. Grese, R.P., Cerny, R.L., Gross, M.L.: Metal Ion-Peptide Interactions in the Gas Phase: A Tandem Mass Spectrometry Study of Alkali Metal Cationized Peptides. *J. Am. Chem. Soc.* **111**, 2835–2842 (1989)
39. Grese, R.P., Gross, M.L.: Gas-Phase Interactions of Lithium Ions and Dipeptides. *J. Am. Chem. Soc.* **112**, 5098–5104 (1990)
40. Teesch, L.M., Adams, J.: Fragmentations of Gas-Phase Complexes between Alkali Metal Ions and Peptides: Metal Ion Binding to Carbonyl Oxygens and Other Neutral Functional Groups. *J. Am. Chem. Soc.* **113**, 812–820 (1991)
41. Leary, J.A., Williams, T.D., Bott, G.: Strategy for Sequencing Peptides as Mono- and Dilithated Adducts Using a Hybrid Tandem Mass Spectrometer. *Rapid Commun. Mass Spectrom.* **3**, 192–196 (1989)
42. Rodriquez, C.F., Fournier, R., Chu, I.K., Hopkinson, A.C., Siu, K.W. M.: A Possible Origin of $[M - nH + mX]^{(m-n)+}$ Ions (X=alkali metal ions) in Electrospray Mass Spectrometry of Peptides. *Int J Mass Spectrom* **192**, 303–317 (1999)
43. Wu, L., Meurer, E.C., Young, B., Yang, P., Eberlin, M.N., Cooks, R. G.: Isomeric Differentiation and Quantification of α, β-Amino Acid-Containing Tripeptides by the Kinetic Method: Alkali Metal-Bound Dimeric Cluster Ions. *Int J Mass Spectrom* **231**, 103–111 (2004)
44. Nezu, Y., Miyazaki, M., Sugiyama, K., Kajiwara, I.: Dimethoxypyrimidines as Novel Herbicides. Part 1. Synthesis and Herbicidal Activity of Dimethoxyphenoxyphenoxypyrimidines and Analogues. *Pestic Sci* **47**, 103–113 (1996)
45. Nezu, Y., Miyazaki, M., Sugiyama, K., Wada, N., Kajiwara, I., Miyazawa, T.: Dimethoxypyrimidines as Novel Herbicides. Part 2. Synthesis and Herbicidal Activity of *o*-Pyrimidinylsalicylates and Analogues. *Pestic Sci* **47**, 115–124 (1996)
46. Wang, H.Y., Zhang, X., Guo, Y.L.: Using Tandem Mass Spectrometry to Predict Chemical Transformations of 2-Pyrimidinyloxy-*N*-Arylbenzyl Amine Derivatives in Solution. *J. Am. Soc. Mass Spectrom.* **17**, 253–263 (2006)
47. Warren, L.A., Smiles, S.: Iso-β-Naphthol Sulphide. *J. Chem. Soc.* 956–963 (1930)
48. Frisch, M.J., Trucks, G.W., Schlegel, H.B., Scuseria, G.E., Robb, M.A., Cheeseman, J.R., Zakrzewski, V.G., Montgomery, J.A., Stratmann, R.

E., Burant, J.C., Dapprich, S., Millam, J.M., Daniels, A.D., Kudin, K. N., Strain, M.C., Farkas, O., Tomasi, J., Barone, V., Cossi, M., Cammi, R., Mennucci, B., Pomelli, C., Adamo, C., Clifford, S., Ochterski, J., Petersson, G.A., Ayala, P.Y., Cui, Q., Morokuma, K., Malick, D.K., Rabuck, A.D., Raghavachari, K., Foresman, J.B., Cioslowski, J., Ortiz, J.V., Stefanov, B.B., Liu, G., Liashenko, A., Piskorz, P., Komaromi, I., Gomperts, R., Martin, R.L., Fox, D.J., Keith, T., Al-Laham, M.A., Peng, C.Y., Nanayakkara, A., Gonzalez, C., Challacombe, M., Gill, P. M.W., Johnson, B., Chen, W., Wong, M.W., Andres, J.L., Gonzalez, C., Head-Gordon, M.E., Replogle, S., Pople, J.A.: Gaussian 03. Gaussian Inc, Pittsburgh, PA (2003)

49. Zhou, Y.P., Pan, Y.J., Cao, X.J., Wu, J., Jiang, K.Z.: Gas-Phase Smiles Rearrangement Reactions of Deprotonated 2-(4,6-Dimethoxypyrimidin -2-Ylsulfanyl)-N-Phenylbenzamide and Its Derivatives in Electrospray Ionization Mass Spectrometry. *J. Am. Soc. Mass Spectrom.* **18**, 1813–1820 (2007)
50. Larrivee, M.L., Allison, J.: Gas-Phase Chemistry of Li^+ with Monofunctional and α,ω-Bifunctional Organic Molecules. How Does the Presence of a Second Functional Group Enhance Reactivity? *J. Am. Chem. Soc.* **112**, 7134–7140 (1990)
51. Kuck, D., Bather, W., Grutzmacher, H.F.: Intramolecular Ring-to-Ring Proton Transfer in Gaseous (ω-Phenylalkyl)Benzenium Ions. *J. Am. Chem. Soc.* **101**, 7154–7157 (1979)
52. Kuck, D., Ingemann, S., de Koning, L.J., Grutzmacher, H.F., Nibbering, N.M.M.: Proton Exchange between Arenium Ions and Arenes in the Gas Phase. *Angew. Chem. Int. Ed Engl.* **24**, 693–695 (1985)
53. Filges, U., Grutzmacher, H.F.: Fragmentations of Protonated Benzaldehydes via Intermediate Ion/Molecule Complexes. *Org Mass Spectrom* **21**, 673–680 (1986)
54. Filges, U., Grutzmacher, H.F.: Fragmentations of Protonated Acetophenones via Intermediate Ion-Molecule Complexes. *Org Mass Spectrom* **22**, 444–450 (1987)
55. Filges, U., Grutzmacher, H.F.: Proton Migration in Naphthalenium Ions via σ and π Complexes. *Int J Mass Spectrom Ion Process* **83**, 93–109 (1988)
56. Grutzmacher, H.F., Thielking, G.: Internal Reactions of Ion-Neutral Complexes from Some Disubstituted Protonated Benzaldehydes and Acetophenones. *Org Mass Spectrom* **23**, 397–405 (1988)
57. Attina, M., Cacace, F., Ricci, A.: Gas-Phase Alkylation of Phenyltrimethylsilanes. Using the Trimethylsilyl Group to Probe Proton Shifts in Gaseous Arenium Ions. *J. Am. Chem. Soc.* **113**, 5937–5942 (1991)
58. Thielking, G., Filges, U., Grutzmacher, H.F.: Remote Fragmentations of Protonated Aromatic Carbonyl Compounds via Internal Reactions in Intermediary Ion-Neutral Complexes. *J. Am. Soc. Mass Spectrom.* **3**, 417–426 (1992)
59. Kuck, D.: Half a Century of scrambling in organic ions: complete, incomplete, progressive and composite atom interchange. *Int J Mass Spectrom* **213**, 101–144 (2002)
60. Kuck, D.: In: Nibbering, N.M.M. (ed.) The Encyclopedia of Mass spectrometry. Topic B16, vol. 4, pp. 229–242. Elsevier, Amsterdam (2005)
61. Kuck, D.: In: Nibbering, N.M.M. (ed.) The Encyclopedia of Mass spectrometry. Topic B20, vol. 4, pp. 270–286. Elsevier, Amsterdam (2005)
62. Kuck, D.: Scrambling versus Specific Processes in Gaseous Organic Ions during Mass Spectrometric Fragmentation: Elucidation of Mechanistic Origins by Isotope Labeling—an Overview. *J. Label. Compd. Radiopharm.* **50**, 360–365 (2007)
63. Kirchhoff, D., Grutzmacher, H.F., Grutzmacher, H.: Trends in the Periodic System: the Mass Spectrum of Dimethylphenyl Phosphane and a Comparison of the Gas Phase Reactivity of Dimethylphenyl Pnictogene Radical Cations $C_6H_5E(CH_3)_2^{\cdot+}$, (E=N, P, As). *Eur J Mass Spectrom* **15**, 131–144 (2009)
64. Guo, C., Wan, J.P., Hu, N., Jiang, K.Z., Pan, Y.J.: An Experimental and Computational Investigation on the Fragmentation Behavior of Enaminones in Electrospray Ionization Mass Spectrometry. *J. Mass Spectrom.* **45**, 1291–1298 (2010)
65. Kuck, D.: Mass Spectrometry of Alkylbenzenes and Related Compounds. Part II. Gas Phase Ion Chemistry of Protonated Alkylbenzenes (Alkylbenzenium Ions). *Mass Spectrom. Rev.* **9**, 583–630 (1990)